Transmembrane S1 Mutations in *CNGA3* from Achromatopsia 2 Patients Cause Loss of Function and Impaired Cellular Trafficking of the Cone CNG Channel

Kirti A. Patel,[1] *Kristen M. Bartoli,*[1] *Richard A. Fandino,*[1] *Anita N. Ngatchou,*[2] *Gustaw Woch,*[1] *Jannette Carey,*[2] *and Jacqueline C. Tanaka*[1]

Purpose. Achromatopsia 2, an inherited retinal disorder resulting in attenuation or loss of cone function, is caused by mutations in the α subunit of the cone cyclic nucleotide-gated (CNG) channel gene *CNGA3*. Examination of mutations that cluster in the first transmembrane segment of the protein may provide insight into its role in CNG channel structure, function, biogenesis, and pathophysiology.

Methods. The human *CNGA3* gene was tagged at the C terminus with green fluorescent protein. Four mutations, Y181C, N182Y, L186F, and C191Y, were expressed in human embryonic kidney cells. Protein expression was evaluated with immunoblot analysis and cellular localization was determined by immunocytochemistry. Channel function was evaluated by patch-clamp electrophysiology.

Results. All the mutations result in loss of channel function, as determined by the failure of cGMP to activate wild-type currents in excised patches. Full-length mutant proteins were synthesized but retained in the endoplasmic reticulum. Glycerol treatment did not rescue channel function nor did coexpression with CNGB3, a subunit of native hetero-tetrameric cone channels. A control mutant, C191S, exhibited cGMP current activation with significantly reduced cooperativity, suggesting that mutations in the first transmembrane domain alter in inter- or intrasubunit communication.

Conclusions. The results implicate the first transmembrane segment in both maturation and function of CNG channels. The defects are not reversed with glycerol, a chemical chaperone that rescues channel function in some channelopathies. Molecular analysis of achromatopsia 2 mutations may be useful in evaluating potential therapeutic approaches for treatment of this channelopathy. (*Invest Ophthalmol Vis Sci.* 2005;46: 2282–2290) DOI:10.1167/iovs.05-0179

Cyclic nucleotide-gated (CNG) ion channels are tetrameric integral proteins of the plasma membrane that gate in response to light-induced changes in intracellular cyclic nucleotides.[1] Unlike the related potassium channels (Kv) that are gated by voltage, CNG channels are relatively nonspecific with respect to the ions they admit, and their gating is relatively insensitive to voltage.[2] The functionally intermediate hyperpolarization and nucleotide-gated channels (HCN) gate in response to both nucleotides and voltage.[3] The domain, subdomain, and subunit organization of channel proteins reflect the fact that stimulus and response result from communication, both within and among polypeptide chains. A central transmembrane domain houses the functions of voltage-sensing, gating, pore formation, and ion selectivity. In the large Kv family of ion channels that include CNG channels, flanking intracellular domains mediate subunit assembly and enable modulation by various stimuli. [1,4–6] The nucleotide-binding domain of CNG channel proteins has a canonical structure found in a wide range of otherwise unrelated cyclic nucleotide-binding proteins[7–9] and, as in many of those cases, is linked to a region housing a multimerization function.[10]

Mutations in ion channels and other membrane receptors are increasingly being associated with diseases of the nervous system through advances in human molecular genetics.[11] Achromatopsia describes a spectrum of inherited retinal disorders involving attenuation or loss of color vision.[12,13] Mutations in the cone CNG channel gene *CNGA3* result in attenuation or loss of cone function in achromatopsia 2 (MIM 216900; Mendelian Inheritance in Man, Bethesda, MD). About half of known patients with achromatopsia have mutations that map to the integral membrane domain, with clusters in the first and fourth membrane-spanning helices and the pore itself.[14–16] The first membrane-spanning helical region S1 has not been implicated previously in channel permeation, gating, or subunit assembly. This cluster of disease mutations Y181C, N182Y, L186F, and C191Y thus provides a lens through which to focus questions about the role of the transmembrane region in protein structure, function, biogenesis, pathophysiology, and evolution. The results reported herein indicate both aberrant channel function and defective intracellular trafficking of these mutant proteins, and suggest a role for the first membrane-spanning region in both channel function and biogenesis.

Methods

Alignment of the S1 Domain

Multiple alignment of A-type CNG channel S1 regions was performed with Clustal W (http://www.ebi.ac.uk/clustalw/multiple sequence alignment program provided by European Bioinformatics Institute, European Molecular Biology Laboratory, Heidelberg, Germany). B-type subunits were not included. A-type subunits include CNGA1 from rod photoreceptors, CNGA2 from olfactory cilia, and CNGA3 from cone photoreceptors. The alignment is available from the corresponding author by request. The helical wheel projection was generated with free-wear developed by Marcel Turcotte at the University of Ottawa, Ontario, Canada (http://www.site.uottawa.ca/~turcotte/resources/HelixWheel/).

From the [1]Center for Biotechnology, Temple University, Philadelphia, Pennsylvania; and the [2]Chemistry Department, Princeton University, Princeton, New Jersey.

Supported by National Eye Institute Grant EY06640 (JCT), National Science Foundation Grant MCB 01-36094(JC), and an HHMI award to Temple University to undergraduate research (KMB).

Submitted for publication February 10, 2005; revised March 13, 2005; accepted March 25, 2005.

Disclosure: **K.A. Patel**, None; **K.M. Bartoli**, None; **R.A. Fandino**, None; **A.N. Ngatchou**, None; **G. Woch**, None; **J. Carey**, None; **J.C. Tanaka**, None

The publication costs of this article were defrayed in part by page charge payment. This article must therefore be marked "*advertisement*" in accordance with 18 U.S.C. §1734 solely to indicate this fact.

Corresponding author: Jacqueline C. Tanaka, Center for Biotechnology, School of Science and Technology, Temple University, Philadelphia, PA 19122; jtanaka@.temple.edu.

Construction of *CNGA3* Mutants

Human *CNGA3*, a gift from King-Wai Yau[17] was cloned into a eukaryotic expression vector (pCMV Script; Stratagene, La Jolla, CA). All mutations for this project were introduced into *CNGA3* with a mutagenesis program (Quickchange; Stratagene). After verification of the sequence of the region containing the mutations, transfected cells were screened for cGMP-activated currents.

The *CNGA3-GFP* cDNA was generated by introducing an *Age*I restriction site at the 3′ end of the *CNGA3* gene to eliminate the stop site. A *Kpn*I restriction site was introduced at the 3′ end of the GFP gene in pEGFP-N1 (BD-Clontech, Palo Alto, CA) and was used to clone *GFP* onto *CNGA3* in the vector (pCMV Script; Stratagene). Ligation of the *Age*I restriction site in the multiple cloning region at the 5′ end of the *GFP* gene added an additional two residues, Ala and Thr, before the initial Met of the *GFP*. The entire wild-type *CNGA3-GFP* gene was sequenced. All mutations were introduced into *CNGA3-GFP* (Quickchange; Stratagene) and sequenced through the region undergoing mutagenesis.

Heterologous Expression of *CNGA3* Mutants

The human embryonic kidney cell line tSA201 was used for *CNGA3* expression studies, as described previously.[18] The cells were transfected with one of two transfection reagents (Fugene 6; Roche Applied Science, Indianapolis, IN, or Lipofectamine; Invitrogen-Gibco, Grand Island, NY) with ~2.5 μg of DNA, approximately 24 hours after plating in 35-mm dishes of ~250,000 cells. Transfected cells were patched 3 to 4 days after transfection. In early experiments with CNGA3, ~1 μg of cDNA encoding soluble enhanced green fluorescent protein (eGFP) was cotransfected for cell selection. These cells were studied no later than 48 hours after transfection because the fluorescence decayed rapidly. For heteromeric channel expression studies, 4 μg of CNGB3 was used in addition to 2 μg of CNGA3. Western blot analysis and immunocytochemistry of CNGA3-GFP and GFP-tagged mutant proteins were conducted ~48 hours after transfection. Mouse CNGB3 was a gift from Andrea Gerstner (Institut für Pharmakologie und Toxikologie, Technische Universität München, Munick, Germany).[19]

Electrophysiology

Inside-out patches were excised from tSA201 cells with a glass electrode, as previously described.[20] The bath and pipette solution contained 120 mM NaCl, 2 mM EGTA, 2 mM EDTA, and 5 mM HEPES at pH 7.3. Patches were obtained by using electrodes with resistances in the range of 3.0 to 3.5 MΩ. A series of 250-ms voltage pulses were applied in 10- or 20-mV steps from −100 to +100 mV. Currents were analyzed at +80 and −80 mV on computer (ClampFit 9.0 software; Axon Instruments, Foster City, CA). Although none of the mutant CNGA3 channels produced current increases as large as those of the wild-type CNGA3 channels, some mutant channel patches responded to cGMP application with increases in current noise. These current increases were suggestive of patches with few channels and channels with aberrant behavior compared with wild-type channels.

Dose–response relations for heteromeric channels formed from co-transfecting CNGB3 with either CNGA3 or C191S mutant CNGA3 were determined by plotting the fraction of current activated as a function of the nucleotide concentration at −80 mV. The normalized currents were fitted as a function of the test concentration using the Hill equation:

$$\text{Fraction of current} = I_{nor}/[1 + (K_{0.5}/L)^n]$$

with a nonlinear Levenberg-Marquardt fitting routine performed on computer (TableCurve; SPSS, Chicago, IL), where I_{nor} is the normalized maximal response, L is the ligand concentration, $K_{0.5}$ is the concentration at 50% of the I_{nor}, and n is the cooperativity index.

Fluorescence Localization and Immunocytochemistry

To characterize the fluorescence distribution of the CNGA3-GFP mutant proteins, cells grown on coverslips were fixed 48 hours after transfection by using 4% paraformaldehyde in phosphate-buffered saline (PBS). The coverslips were washed three times in PBS and mounted onto a glass slide with antifade medium (VectaShield; Vector Laboratories, Inc., Burlingame, CA). Cells were viewed at 100× with a fluorescence microscope (Nikon, Melville, NY). At least five coverslips from different transfections were used for each analysis. All fluorescent cells in a field were evaluated for the presence or absence of Golgi-like dense fluorescent regions. The results were plotted to evaluate the significance of the differences between the wild-type and mutant channels.

The endoplasmic reticulum (ER) was localized by using glucose-regulated protein (GRP94) as a marker. GRP94 belongs to a family of Hsp90 molecular chaperones. This soluble protein contains a COOH-terminal tetrapeptide that causes it to be retained in the ER. For the colocalization studies, cells on coverslips were fixed 48 to 63 hours after transfection with 4% paraformaldehyde in PBS for 15 minutes. The coverslips were exposed to 95% ethanol for 5 minutes, washed three times in PBS for 5 minutes, and treated with blocking solution containing 0.1% Tween and 1% normal goat serum in PBS for 1 hour at room temperature. To colocalize the CNGA3-GFP and the Grp94 proteins, the coverslips were treated 2 hours in primary Grp94 (Stressgen Biotechnologies, San Diego, CA) antibody (1:300) in blocking solution. Cells were washed three times in PBS and treated with a rhodamine-conjugated secondary antibody (Molecular Probes, Eugene, OR).

Immunoblot Analysis of Protein Expression

Cells were grown in 35-mm dishes. At ~48 hours after transfection, cells were rinsed with ice-cold PBS, removed using a rubber cell scraper, and lysed with ~50 μL of radioimmunoprecipitation (RIPA) buffer containing 10 mM Tris (pH 7.2), 1% Triton X-100, 1% sodium deoxycholate, 150 mM NaCl, 0.1% SDS, and protease inhibitors in 1 mM phenylmethylsulfonyl fluoride (PMSF), 20 μM leupeptin, and 0.5 μM aprotinin at 4°C. The cell lysate was incubated on ice for ~15 minutes, followed by dispersion of the cells with a small syringe and 21-gauge needle. The cell lysate was centrifuged for ~4 minutes and the pellet discarded. Protein concentrations were determined with a Bradford assay. The samples were retained on ice, mixed with prewarmed 2× loading buffer and immediately loaded onto the gel. Standard SDS-PAGE and transfer buffers were used for running the gel and for transferring the gel to a 0.45-μm pore nitrocellulose membrane (Schleicher & Schuell, Keene, NH) at ~70 mA. The membrane was blocked in 5% dry milk in washing buffer containing Tween (0.05%)-Tris buffered saline (TTBS) for 2 hours at room temperature, followed by an overnight incubation with primary anti-GFP antibody (Sigma-Aldrich) in TTBS blocking solution at the indicated dilutions (see Fig. 4). The membrane was washed and incubated with a horseradish peroxidase (HRP)–labeled secondary antibody in TTBS blocking solution for 45 minutes. The membrane was subjected to another set of washes, followed by visualization using the enhanced chemiluminescence kit (ECL; Amersham Life Sciences, Inc., Piscataway, NJ).

Results

Sequence and Structural Analysis to Define S1

There are no high-resolution structures of CNG channel family members available at present that would directly define the transmembrane regions of the channels. Previous alignments placed C191 in the extracellular loop between S1 and S2.[14,21–23] Based on this alignment, the cluster of achromatopsia mutations that include Y181C, N182Y, L186F, and C191S would traverse different domains of the channel. Examination of the ~25 presently known sequences of photoreceptor chan-

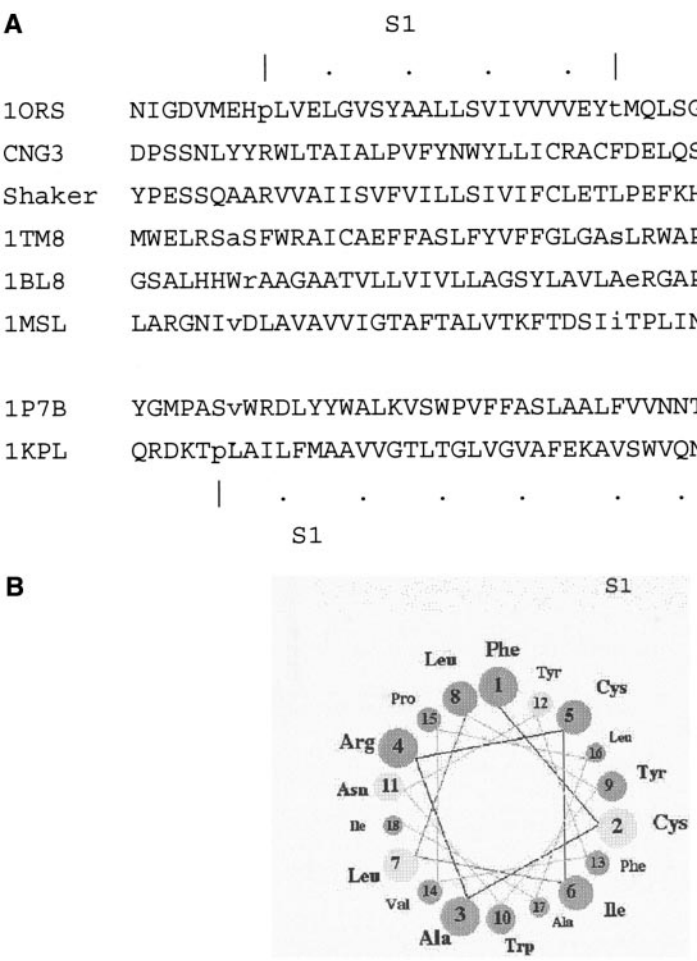

FIGURE 1. (**A**) Common features in S1 regions of distantly related channel proteins. One-letter amino acid codes are used. For known crystal structures (pdb codes [provided by the Research Collaboratory for Bioinformatics] are given: 1ORS, voltage-activated potassium channel of *Aeropyrum pernix*; 1TM8, aquaporin 0 of *Bos taurus*; 1BL8, potassium channel of *Streptomycetes lividans*; 1MSL, mechanosensitive channel of *Mycobacterium tuberculosis*; 1P7B, inward-rectifier potassium channel of *Burkholderia pseudomalaria*; 1KPL, chloride channel of *Salmonella typhimurium*). *Lowercase letters*: N- and C-terminal residues of the S1 helix. *Right*: the protein sequence number of the last residue shown. *Lowercase letters*: N-terminal residues of the S2 helix, which is truncated (. . .) or distal to (>) the sequences shown. Helix limits in 1ORS or 1KPL, respectively, are emphasized by *bars above* or *below* the sequences, and helix positions 5, 10, 15, and so on, are marked (.). (**B**) Helical wheel projection CNGA3 S1. Residues assigned to the helix based in (**A**), are displayed in a view looking down the helix axis from the outer membrane surface. Thus, F192, the last residue assigned to the helix, is the first residue of the projection, labeled residue 1, at the *top*. The helix disappears into the page after the 18th residue, L175. Residues mutated in achromatopsia that were studied in this work are encircled in *light gray*: Y182 (residue 12 in this view), N182 (residue 11), L186 (residue 7), and C191 (residue 2).

nel A-type subunits revealed that the mutations studied in this work are highly conserved. Within this family, sequence identities in the S1 region were very high, producing an ungapped and unambiguous multiple alignment with residues 160 to 200 of human CNGA3. Several positions displayed no residue variability, and many others are restricted to two or three residues of similar functional group type. Residue variability in the vicinity of the achromatopsia 2 mutations that we studied is particularly narrow, and the sites of mutation are among the most highly restricted.[14] For example, from Pro178 to Phe192 inclusive, the consensus sequence is (P,A)(V,S,I)(F,M,L)(*Y*)(*N*)(W,L,I)(Y,C,T,V,I)(L,M,I,F)(*L*,I,V)(I,V,)(C,A,G)(R)(A)(*C*,V)(F,Y), with sites of the studied mutations in italic.

Ion channel homologues of known structure could, in principle, be used to define the boundaries of the CNGA3 S1 helix and perhaps suggest functional hypotheses for sites involved in the achromatopsia 2 mutations that we studied. In Fig. 1A, the human CNGA3 sequence is compared with six available x-ray crystal structures of distantly related channel proteins. The known structures comprise two groups differing in S1 helix length by approximately seven residues or approximately two helical turns, although sequence homologies between the two groups are too weak to establish where the helix would be extended. Among these structures CNGA3 is most closely related in function to the voltage-dependent potassium channel KvAP from *Aeropyrum pernix* (1ORS), a member of the group with shorter (~24 residues) S1 helices.[24] The sequence homology is too weak to offer a confident alignment that could assign specific residues to S1 of CNGA3; however, the KvAP channel 1ORS can be aligned with the Shaker K^+ channel by homology.[24] This alignment appears to provide a homology bridge between CNGA3 and 1ORS, and to the remaining structures, while still not offering secure endpoints for the S1 helix.

In the six sequences in the top section of Fig. 1A, residues with broadly similar functional group properties cluster within S1. Each S1 region contains two or three contiguous stretches of hydrophobic residues, many of which are β-branched, and these stretches are punctuated by small polar residues. This unusual residue composition bias is reminiscent of glycophorin, the structure of which suggests a key role for the conformationally constrained β-branched residues in helix packing.[25,26] The ends of S1 are marked by clusters of charged and/or polar residues. CNGA3 follows these general patterns, although sequence identities with the other proteins are few. It seems likely that all the achromatopsia mutations that we studied lie in the C-terminal half of S1. However, definitive assignment of the C terminus is impossible, given the very low homology and the fact that helix termini are variable, even in homologous proteins of known structure. Although C191 resides in exon 6, whereas the other three mutations reside in exon 5,[14] the location of helix termini probably reflect local structural constraints and need not reflect exon boundaries. Assignment of the C-terminal end of S1 to Cys191 or Phe192 on the basis of residue properties appears somewhat more secure than assignment of the N terminus, which may be located between Asp157 and Arg171.[25]

The S1 mutations were arranged on a helical wheel diagram starting from the outward-facing C terminus of S1 to examine their disposition and proximity on the helix surface. Fig. 1B shows a view of the resultant helical projection, looking inward from the outer membrane surface down the axis of S1. Thus, the residue assigned as the C terminus of S1, Phe192, is

residue 1 of the projection, which disappears into the page after the 18th residue, Ile175. Considering the entire helix extending back to Asn167, a length similar to that of the known S1 structures, a consistently hydrophobic surface of the helix that might face the lipid bilayer lies at the bottom of the figure (not shown). This surface is bracketed by residues 2 and 7 in the projection, which mark two of the sites of achromatopsia 2 mutations studied here (C191Y and L186F, respectively). Three of the mutations, C191Y, L186F, and N182Y, involve attachment of an aromatic ring to Cβ in place of a smaller or less constrained functional group.

cGMP-Activated Currents in S1 Mutant CNGA3 Channels

The S1 mutations Y181C, N182Y, L186F, and C191Y were engineered in the human CNGA3 gene. In initial experiments, channels were transiently expressed in human embryonic kidney tSA201 cells and selected for patch recording by cotransfecting the cells with a cDNA-encoding soluble GFP. None of the mutants produced normal cGMP-activated currents. By contrast, typical currents in response to saturating concentrations of cGMP were 200 to 2000 pA in excised patch recordings with homo-tetrameric wild-type CNGA3 channels. Currents returned to baseline levels within 2 minutes after cGMP washout (data not shown but similar to Fig. 2, top traces). Failure of the mutants to produce cGMP-activated currents could be due to degradation of the mutant protein before it reaches the plasma membrane, failure of transport to the plasma membrane, misfolded or misassembled subunits, and/or abnormal channel function. To track the mutant channels directly, fusion proteins were generated with GFP attached at the C-terminal end of CNGA3. Recent studies of rod CNGA1 and CNGB1 subunits showed that CNG subunits could be tagged in this manner with no apparent change in protein expression or channel function.[27,28] All data reported herein were collected from GFP-fusion channels.

Channel function was evaluated with patch-clamp electrophysiological current recordings from transfected tSA201 cells, by using excised, inside-out membrane patches. Figure 2 shows current recordings at +80- and −80-mV holding potentials before (left) and during (middle) 500 μM cGMP exposure, and after washout of cGMP (right). A wild-type CNGA3-GFP channel response is shown in the top row. The current increased from the background level to ~700 pA with the application of cGMP and rapidly returned with a 1-minute washout. Representative traces for the S1 mutant channels are shown below the wild-type traces in Figure 2. None of the mutant current recordings showed wild-type channel behavior, with large, stable cGMP-activated currents that were rapidly reversible and similar in magnitude at positive and negative potentials. Current traces for Y181C, N182Y, and L186F showed small, if any, response to cGMP application. The current traces for C191Y showed a large, noisy current at positive potentials with cGMP exposure but the current at negative potentials was quite small. This outward rectification in the current–voltage relation is different from the relatively linear current–voltage relation of the wild-type CNGA3 channel shown in the top panel. Although the current in this C191Y patch showed a nearly complete reversal with washout of cGMP, dose–response relations were not obtained, because the patches had relatively short lifetimes compared with wild-type channel patches. Small increases in the current noise or the mean current were seen in some of the patches expressing N182Y and C191Y channels, suggesting a current increase with cGMP; however, these currents were too small to analyze.

Because cone CNG channels are heterotetrameric, currents were examined in cells transfected with both CNGA3 and CNGB3 subunits to replicate more closely the cone channel composition. None of the mutant channels exhibited the stable, symmetric currents seen with wild-type channels (data not shown) indicating that the CNGB3 subunit was unable to rescue CNG channel function.

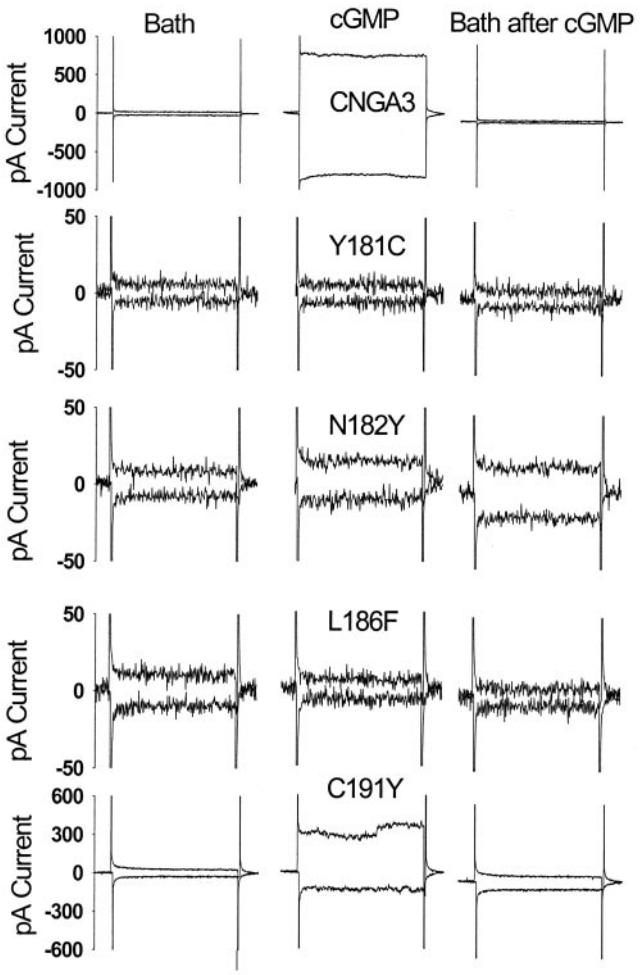

Figure 2. Patch-clamp currents of mutant channel function. Each panel shows current traces versus time at two voltages. *Left*: the initial bath current recording; *middle*: the current in the presence of 500 μM cGMP; and *right*: the bath current after washout from cGMP exposure. The negative-current traces were recorded with the membrane potential clamped at 0 mV for 20 ms and then stepped to −80 mV for 200 ms and returned to 0 mV. Capacitative currents, not subtracted, appear as large current impulses with the voltage. The positive currents were recorded with the same protocol and the holding potential at +80 mV. Note the different current scales among the panels. Currents from the patches shown are representative of each mutant. From 17 to 40 patches were examined for each mutant homomeric channel; an additional 12 to 15 patches were examined for each mutant coexpressed with the CNGB3 subunit, not shown.

Effect of the Nondisease Mutant C191S

A conserved cysteine residue in the S1-region of the bovine rod CNGA1 channel, C186, has been examined in an earlier study. This cysteine residue, which aligns with C191 in human CNGA3, was mutated to serine to produce a cysteineless mutant for cysteine-scanning studies.[29] No abnormalities were reported in channel function for the CNGA1 cysteineless mutant. The results with the rod mutant suggest that replacing C191 in the cone channel with serine may be tolerated, even though C191Y produces a nonfunctional CNGA3 channel. To

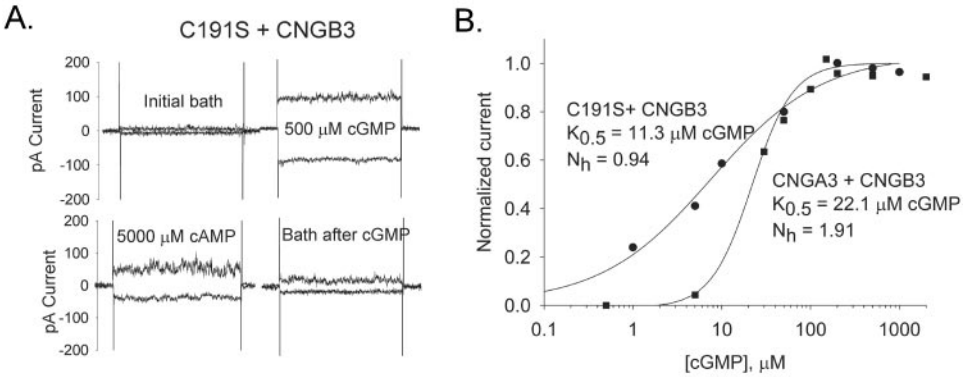

FIGURE 3. Examination of nondisease mutant C191S. (**A**) Currents from heteromeric channels formed from C191S and CNGB3 subunits. Current traces at −80 and +80 mV are shown under conditions to those in Figure 2. Note the large current fluctuations at positive potentials for this mutant, apparent in the upper current traces for all conditions. All patches from heteromeric channels with this mutation showed this characteristic. Currents at −80 mV were used to determine the cAMP efficacy and cGMP dose–response curve. (**B**) The cyclic GMP dose–response curve for C191S heteromeric channels. Dose–response relations are shown for currents from a single patch at −80 mV. Current versus cGMP concentration data were fitted using a nonlinear dose–response relation (see the equation).

investigate this possibility, a C191S mutant was generated in the human CNGA3. The homomeric C191S channels responded to cGMP with small, noisy increases in current that were reversible for all responsive patches (data not shown). Similar to results with C191Y, the currents at positive potentials were often much larger and noisier than those at negative holding potentials.

Coexpression of C191S with CNGB3 resulted in larger currents than those from homomeric C191S channels. Figure 3A shows current traces from cells transfected with both C191S and CNGB3 subunits. The larger currents recorded from heteromeric channels permitted a measurement of the nucleotide selectivity, a characteristic of CNG channels from different cell types. In cone CNG channels, cAMP is a weak agonist activating from 2% to 16% of the maximum cGMP-activated current in homomeric channel patches and from 20% to 58% of maximum current in patches excised from cells after cotransfection with both CNGA3 and CNGB3 subunits.[19,27,30,31] In cells transfected with both C191S and CNGB3, cAMP efficacy was 30% and 28% in two patches. Comparable efficacy values from cells expressing the wild-type subunits A3 and B3 were 36% ± 0.12% (SEM; $n = 6$) and for homomeric CNGA3 channels, 10.5% ± 0.12% ($n = 9$). The fractional currents generated by cAMP suggest that the C191S mutant channels exhibit the nucleotide selectivity expected of cone CNGA3 channels.

Dose–response curves for cGMP were measured in three C191S heteromeric channel patches at −80 mV. A representative dose–response relationship is shown in Figure 3B. Large current noise (apparent in the top traces at +80 mV for 500 μM cGMP and 5 mM cAMP in Fig. 3A) precluded dose–response determinations at positive potentials. The average $K_{0.5}$ for three patches is 26.4 μM ± 8.0 SEM cGMP and the cooperativity is 0.86 ± 0.18 (SEM equation; $n = 3$). For comparison, the average $K_{0.5}$ for wild-type heteromeric channels is 22.7 ± 2.2 μM (SEM) with a cooperativity of 1.9 ± 0.15 (SEM; $n = 6$). Although the molecular origins of cooperativity in CNG channel gating are not well understood, the significantly broader dose–response curves indicate that the C191S mutation alters inter- or intrasubunit interactions involved in cooperative nucleotide activation of the channel.

Comparison of Wild-Type and S1 Mutant Protein Expression

CNGA3 protein expression in transfected cell lysates was next examined using immunoblot analysis with an anti-GFP antibody. These experiments address the possibility that the S1 mutations may lead to misfolding and proteolysis of mutant protein, which could account for the small, aberrant cGMP-activated currents. tSA201 cells were transfected with wild-type or S1 mutant CNGA3-GFP cDNAs and harvested ~48 hours after transfection. Cell lysates were subjected to PAGE and immunoreacted with an anti-GFP antibody. Results from a representative experiment are shown in Figure 4. Cell lysates from CNGA3-GFP produced a high-molecular-mass diffuse band at ~108 kDa and more focused, intense staining of two lower-molecular-mass bands corresponding to ~100 and ~97 kDa. Cell lysates from each of the S1 mutants exhibited the bands at 100 and 97 kDa; however, none of them expressed the diffuse high-molecular-mass species seen in the wild-type protein. This pattern is consistent with recent data from Faillace et al.[32] who showed the high-molecular-mass band to be the mature, fully glycosylated form of the channel. Although we conclude that the S1 mutant channels fail to mature prop-

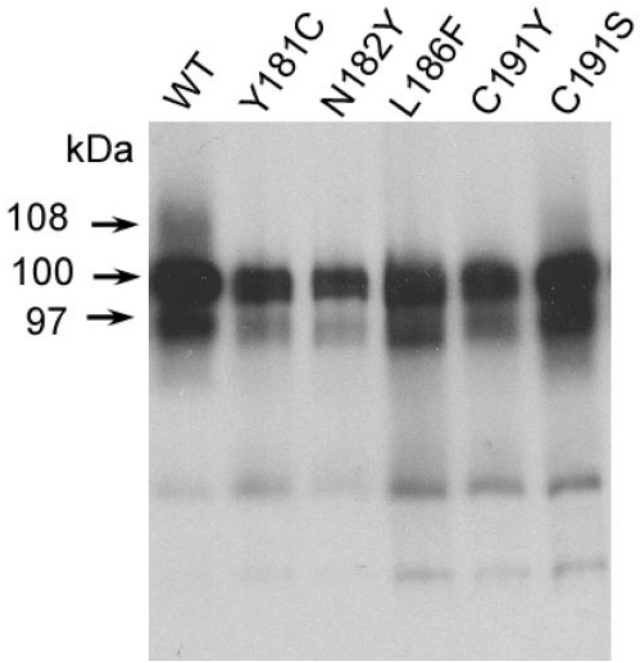

FIGURE 4. Immunoblot of wild-type and mutant proteins. Cell lysates were examined from transiently transfected tSA201 cells expressing wild-type or mutant GFP-labeled CNGA3 proteins 48 hours after transfection. The 7.5% acrylamide gel was run until only the two largest molecular mass standards remained, to visualize the closely migrating bands. The mutant channel lanes are indicated. Approximately 20 μg of the wild-type channel and C191S total lysate protein was loaded and ~25 μg of total lysate protein was loaded for the S1 mutants. The wild-type GFP-tagged protein has a calculated molecular mass of 106 kDa. Primary antibody was a monoclonal anti-GFP at 1:8000; secondary antibody 1:10,000.

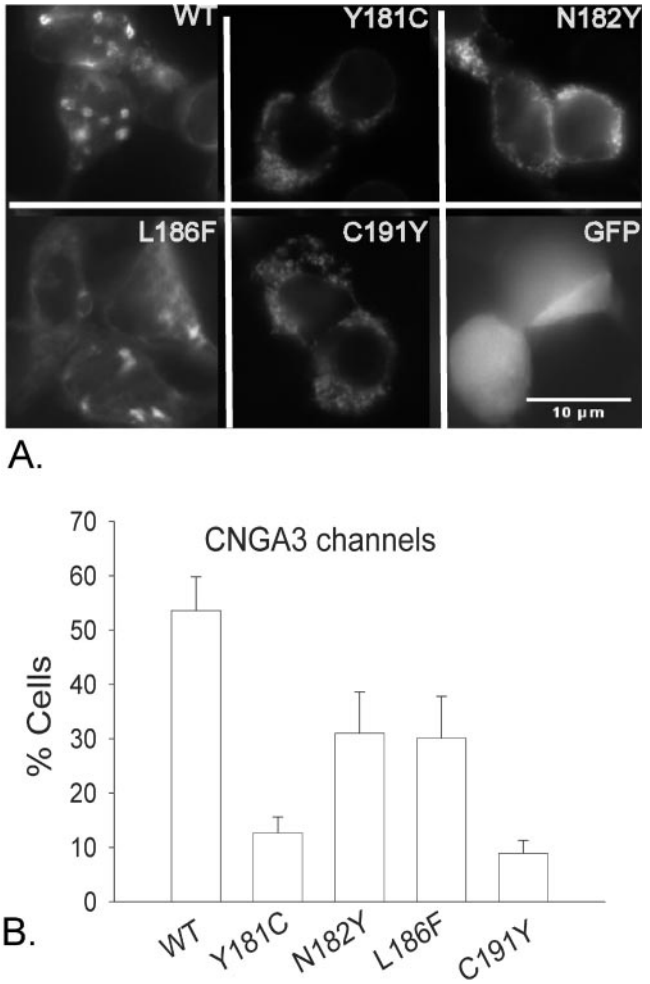

FIGURE 5. Cellular distribution of the wild-type and mutant CNGA3 channels. (**A**) Homomeric channel expression showing different cellular trafficking of S1 mutants. Cells transfected with eGFP-tagged CNGA3 (WT) showed a pattern of fluorescence with predominant focal and membrane distribution. By contrast, the mutant channels showed fewer localized regions of fluorescence with diffuse cell staining throughout the extranuclear regions. *Bottom right*: expression of soluble GFP, shown for comparison. (**B**) Histogram of focal region localization of fluorescence in cells expressing wild-type or S1 mutant channels. Fields of cells were examined from different transfections to evaluate the pattern of fluorescence distribution for the various channels. Data were collected for 400 to 800 cells and expressed as the fraction expressing focal-type staining.

erly with respect to their expected glycosylation pattern, this glycosylation defect alone is unlikely to account for the loss of channel function, since Faillace et al.[32] replaced the ^{357}N (in the bovine CNGA3 equivalent to human ^{339}N), the residue responsible for channel glycosylation, with glutamine and found that wild-type channel function was retained.[32] The immunoblot confirms that full-length mutant proteins were synthesized. Although all samples showed one or two fainter bands at higher mobilities, there was no evidence of extensive proteolytic degradation of the S1 mutant proteins.

Cellular Distribution of GFP Fluorescence in WT and S1 Mutant Channels

The GFP tag on the CNGA3 mutant proteins enabled us to monitor their intracellular localization. The images in Figure 5A show typical expression patterns at ~48 hours after transfection in tSA201 cells. The wild-type fluorescence distribution is concentrated in bright focal regions resembling the Golgi apparatus. The fluorescence is weaker in the cells expressing the S1 mutant channels, with few cells exhibiting focal fluorescence. The mutant protein appears to be distributed throughout the extranuclear region. Labeling of soluble GFP is shown for comparison.

To evaluate better the subcellular distribution of CNGA3, a large number (400–800) of cells were examined by fluorescence microscopy. The fraction of cells showing intense focal-type staining is indicated in the histogram in Figure 5B. More than half of the wild-type cells had intense focal regions, whereas Y181C and C191Y had ~10% of the cells with this pattern and N182Y and L186F showed ~30%. Unpaired *t*-test comparisons showed significant differences between cells expressing wild-type and mutant proteins. The changes in cellular distribution in the mutants were not time dependent, since cells were compared up to 5 days after transfection (data not shown). The pattern of diffuse fluorescence distribution throughout the cells suggests that mutant CNGA3 proteins were retained in the ER.

Colocalization of CNGA3-GFP Channels with an ER-Specific Protein

ER retention of the mutant proteins can be investigated with ER-specific antibodies. Subcellular localization was determined with an antibody to glucose regulatory protein Grp94, a highly specific marker for ER.[33] Mutant CNGA3-GFP fusion proteins colocalized with the ER marker, in contrast to wild-type fusion proteins (data not shown for homomeric channel expression). The cellular distribution of GFP-tagged CNGA3 mutants was also examined in cells expressing heteromeric cone channels containing the CNGB3 subunit. The GFP distribution is shown in Figure 6A, left, rhodamine-labeled Grp94-immunofluorescence in the middle, and the merged images on the right. The wild-type protein distribution shows that some of the bright green focal regions labeled with Grp94, whereas others seemed to represent Golgi staining. By contrast, all the S1 mutant proteins showed a predominant fluorescence distribution that overlapped the ER, leading us to conclude that most of the mutant protein is retained in the ER. A histogram of the focal GFP distribution of heteromeric channels (Fig. 6B) indicates a pattern similar to that for homomeric channels (Fig. 5B). This similarity suggests slight differences in cellular processing among the four mutants that are independent of the CNGB3 subunit.

Rescue of Channel Function by Glycerol

The failure of S1 achromatopsia 2 mutant channel proteins to traffic correctly is not unexpected, considering results emerging from other channelopathies. Increasingly, chemical chaperones are found to play a role in correcting defective trafficking. Both the cystic fibrosis transmembrane conductance regulator and aquaporin-2 express fully functional mutant channels in the presence of glycerol or other chemical chaperones[34,35] or with temperature changes.[36] We examined the effects of glycerol on the S1 mutations by adding 7.5% or 10% glycerol to the culture dishes 4 hours after transfection. The fluorescence distribution at 48 hours is summarized in the histogram in Figure 7A. Glycerol treatment decreased the distribution of focal regions of fluorescence in wild-type channels, compared with non–glycerol-treated cells. No significant changes were seen in fluorescence localization with the mutant channels, suggesting that glycerol exposure does not rescue the defective trafficking of these S1 mutants.

Cyclic GMP-activated currents were examined in patches from glycerol-treated cells. Representative traces are shown in

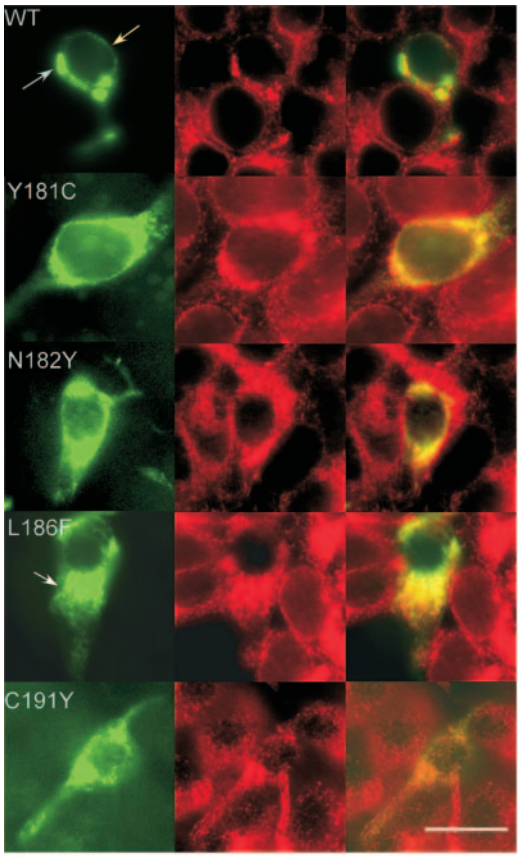

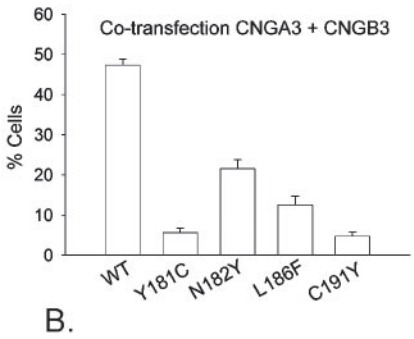

FIGURE 6. **(A)** Colocalization of heteromeric channels with an ER-specific marker shows the mutant channels are retained in the ER. Cells expressing wild-type or mutant CNGA3-GFP were fixed 48 hours after transfection. *Left*: GFP-tagged mutant proteins (*green*). The wild-type cells showed a classic membrane peripheral staining (*yellow arrow*) and focal-type staining (*blue arrow*). The mutant channels show membrane staining as well as predominant diffuse ER staining throughout the cell, L186F (*white arrow*). *Middle*: showed the immunoreactivity of an ER-specific protein, Grp94, (*red*) in the same fields. *Right*: merged images of the *green* and *red* fluorescence signals. **(B)** Histogram of cells containing Golgi-like staining of heteromeric channels. Heteromeric channels were expressed, similar to those shown in (**A**). Fields of cells were examined to evaluate the pattern of staining for the various channels. Note the scale change from (5B).

Figure 7B for Y181C and L186F. Several patches showed large cGMP-responsive currents after glycerol treatment. The Y181C patch selected for this figure showed current reversal with cGMP washout, but Y181C patches were not stable enough to monitor cGMP concentration dependence. Note again the increased noise at positive potentials. The L186F current shown in Figure 7B illustrates several features of glycerol treatment observed with this mutant. Patches showed a small current increase with application of 200 μM cGMP and a further small increase with application of 500 μM cGMP. However, the small currents and relatively short lifetimes prohibited the measurement of dose–response relations. We conclude that glycerol treatment at 7.5% or 10% fails to rescue normal channel function with the S1 mutants.

DISCUSSION

Achromatopsia 2 mutations in the S1 region of the human CNGA3 gene direct attention to residues that are likely to be important in the structure, function, or biogenesis of the channel. None of the four S1-region mutations examined in this study—Y181C, N182Y, L186F, and C191Y—exhibited normal cGMP-activated currents; however, two observations support the conclusion that mutant proteins sometimes reach the cell surface but form functionally defective channels. First, peripheral fluorescence is apparent in some cells, consistent with plasma membrane localization of the full-length protein with the GFP tag on the C terminus. Second, some mutant channels respond to cGMP exposure with an increase in current noise, suggesting the presence of membrane-localized proteins that detect cGMP but fail to gate normally. The nondisease mutant C191S further indicates a defect in channel gating, since its heteromeric channels displayed reduced cGMP cooperativity compared with the wild type. This finding implicates the S1 region in cyclic nucleotide cooperativity for the first time. In addition, the achromatopsia S1 mutants did not achieve a fully glycosylated mature state similar to that of the wild-type protein. However, their functional defects cannot be ascribed solely to aberrant posttranslational maturation, since in wild-type CNGA3, channel function is maintained when the site of glycosylation is mutated.[32] The S1 mutations studied in the present work therefore affect both function and biogenesis, as indicated by retention in the ER and failure to undergo normal glycosylation. A detailed understanding of the mechanisms involved in the defective channel processing will require additional studies that monitor membrane insertion of the S1, protein folding, and subunit assembly.

Studies of human disease mutations have provided a growing list of channelopathies in which protein retention in the ER is now recognized as a major cause.[11] Examples of such trafficking defects occur in the human rod CNGA1 in an autosomal recessive form of retinitis pigmentosa,[37,38] the ΔF508 cystic fibrosis transmembrane regulator, a cAMP-regulated chloride channel[39,40]; a K_{ATP} channel associated with persistent hyperinsulinemic hypoglycemia of infancy[41]; the human ether-a-go-go–related channel causing a congenital long-QT syndrome[42]; and aquaporin-2 channels in nephrogenic diabetes insipidus.[35,43] In some mutant channels, application of a chemical chaperone rescues channel function, indicating that the trafficking defect limits expression of functional channels. In contrast, function of the S1 mutant channels examined in the present study was not rescued by the glycerol treatment used in our experiments.

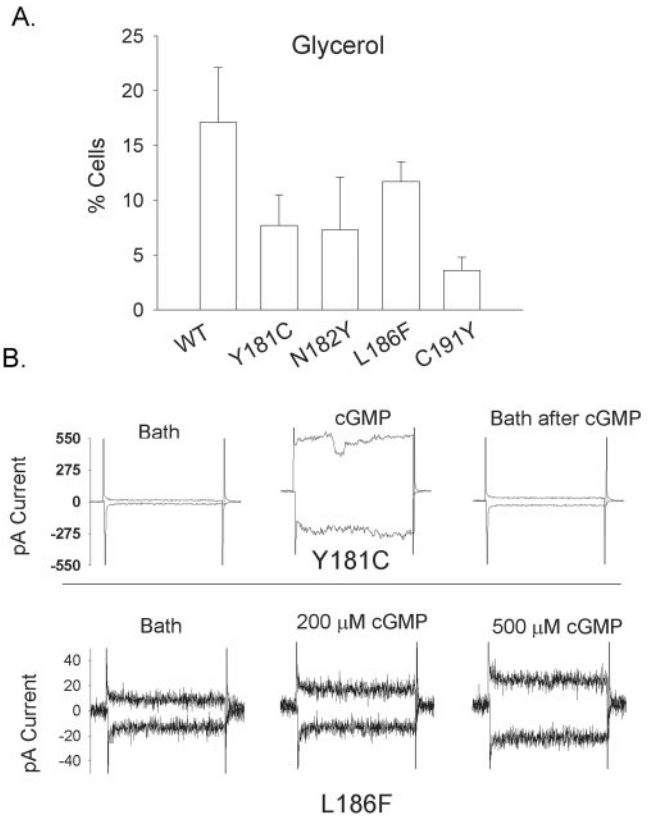

FIGURE 7. Effects of glycerol on CNGA3 expression. (**A**) Differential subcellular distribution of wild-type and mutant CNGA3 fluorescence after glycerol treatment. Glycerol (10%) was added to the media 4 hours after transfection. Cells were fixed as described previously. The increased length of the error bars reflect a smaller number of cells on each coverslip. Loss of cells with glycerol treatment was a consistent feature of the glycerol treatment. The total number of cells counted was >300 for each cell type. Note scale change from previous figures. (**B**) Cyclic GMP-activated currents from Y181C and L186F after glycerol treatment. Currents were recorded from excised patches from glycerol-treated cells. The voltage protocols are the same as in Figure 2. Note the different current scales.

A complexity of achromatopsia 2 is reflected in the wide range of presenting clinical phenotypes noted in the patient screen.[14] Even patients with achromatopsia who have the same mutational changes can show surprisingly large phenotypic variations. In a recent study of two compound heterozygous siblings who inherited T224R located in the intracellular S2-S3 linker and T369S located in the pore,[44] the lack of correlation between disease severity and functional data on the mutant proteins led Trankner et al.[44] to discuss several cone-specific genetic and nongenetic factors that might modulate the clinical profile. Mutations in the S1 region share this pattern of complexity. The C191Y mutation was reported in a compound heterozygote with R277C on the other allele. This individual displayed complete achromatopsia with no cone ERG response. Other compound heterozygotes with mutation N182Y or L186F paired with F547L or R277C, respectively, had no cone ERG responses. The S1 mutations Y181C and C191Y were each also found in homozygous individuals.[14] One homozygote expressing Y181C exhibited reduced cone ERG responses and abnormal color vision, whereas the C191Y homozygote exhibited residual cone ERG responses and residual red color vision. These homozygous phenotypes are unexpectedly mild in view of the current heterologous expression studies showing that neither mutant supports normal channel function even when coexpressed with CNGB3. The fact that all the S1 mutations have both trafficking and functional defects implies that individual variations in protein biogenesis, perhaps influenced by inherited differences in other genes, may greatly affect the disease phenotype.

This study is not the first to report that both functional and trafficking defects map to a single transmembrane segment of CNGA3. A similar observation was made with point mutations introduced into the S4 region of the bovine *CNGA3* gene.[32] Mutations at any of the highly conserved charged residues of S4, including achromatopsia 2 mutations R277C and R283W, caused loss of channel function. Some of these S4 mutants displayed the same kinds of characteristic processing defects seen with the S1 mutants examined in this study: trapping in the ER and failure of the protein to mature after initial glycosylation. In general, more conserved residues were less tolerant of substitution. In contrast, two neutral residues were changed without loss of maturation or function. Even though the CNG channels do not gate in response to voltage changes, the pattern of arginine residues conserved in their S4 regions is a prototypical characteristic of all voltage-gated channels, where these residues are directly implicated in the voltage-sensing mechanism.[45,46] The S4 region probably serves a similarly direct role in the hyperpolarization- and cyclic nucleotide-sensitive channels,[47] which may be evolutionarily intermediate between the CNG and voltage-gated channels.

In CNGA3, the arginine residues of S4 were the most frequent sites of mutation found within the transmembrane domain in the comprehensive screen of patients with achromatopsia by Wissinger et al.,[14] suggesting a possible functional role. The next highest mutation frequencies in the transmembrane domain were found in S1 and in the pore itself. The clustering of disease mutations in S1 and in S4, taken together with the similar channel dysfunctions found in both the S1- and S4-region mutants, suggest that both S1 and S4 have roles in communication between the pore and gating subdomains of the channel. This suggestion would be consistent with recent accessibility mapping in the voltage-gated K^+ channel, which places S1 at the interface between the two functional subdomains.[48]

In summary, detailed analysis of channel function and cellular trafficking for clinically relevant mutant channels will provide insight into the molecular pathophysiology of each of the more than 50 mutations identified in patients with achromatopsia 2. This approach thus provides a system in which to examine potential therapeutic approaches that may increase protein folding, expression, or function for patients with this channelopathy.

Acknowledgments

The authors thank Joel Sheffield and Luis DelValle for help with fluorescence microscopy, the Center for Neurovirology for the use of their fluorescence microscope, and Beatrice Haimovich and Gregg Wells for helpful comments on the manuscript.

References

1. Kaupp UB, Seifert R. Cyclic nucleotide-gated ion channels. *Physiol Rev.* 2002;82:769–824.
2. Zagotta WN, Siegelbaum SA. Structure and function of cyclic nucleotide-gated channels. *Ann Rev Neurosci.* 1996;19:235–263.
3. Biel M, Ludwig A, Zong X, Hofmann F. Hyperpolarization-activated cation channels: a multi-gene family. *Rev Physiol Biochem Pharmacol.* 1999;136:165–182.
4. Roosild TP, Le KT, Choe S. Cytoplasmic gatekeepers of K+-channel flux: a structural perspective. *Trends Biochem Sci.* 2004;29:39–45.
5. MacKinnon R. Potassium channels. *FEBS Lett.* 2003;555:62–65.

6. Kramer RH, Molokanova E. Modulation of cyclic-nucleotide-gated channels and regulation of vertebrate phototransduction. *J Exp Biol*. 2001;204:2921–2931.
7. Weber IT, Steitz TA. Structure of a complex of catabolite gene activator protein and cyclic AMP refined at 2.5 A resolution. *J Mol Biol*. 1987;198:311–326.
8. Scott S-P, Harrison RW, Weber IT, Tanaka JC. Predicted ligand interactions for 3′,5′-cyclic nucleotide-gated channel binding sites: comparison of retina and olfactory binding site models. *Protein Eng*. 1996;9:333–344.
9. Taylor SS, Buechler JA, Yonemoto W. cAMP-dependent protein kinase: framework for a diverse family of regulatory enzymes. *Ann Rev Biochem*. 1990;59:971–1005.
10. Zhong H, Lai J, Yau K-W. Selective heteromeric assembly of cyclic nucleotide-gated channels. *Proc Natl Acad Sci USA*. 2003;100: 5509–5513.
11. Kullmann DM. The neuronal channelopathies. *Brain*. 2002;125: 1177–1195.
12. Wissinger B, Sharpe LT. New aspects of an old theme: the genetic basis of human color vision. *Am J Hum Genet*. 1998;63:1257–1262.
13. Sharpe LT, Stockman A, Jagel H, Nathans J. In: Gegenfurtner K, Sharpe LT, eds. *Night Vision: Basic, Clinical and Applied Aspects*. Cambridge, UK: Cambridge University Press; 1999:3–52.
14. Wissinger B, Gamer D, Jagle H, et al. CNGA3 mutations in hereditary cone photoreceptor disorders. *Am J Hum Genet*. 2001;69: 722–737.
15. Johnson S, Michaelides M, Aligianis IA, et al. Achromatopsia caused by novel mutations in both CNGA3 and CNGB3. *J Med Genet*. 2004;41:e20–e25.
16. Kohl S, Giddings MT, Jagel H, et al. Total colourblindness is caused by mutations in the gene encoding the alpha-subunit of the cone photoreceptor cGMP-gated cation channel. *Nat Genet*. 1998;19: 257–259.
17. Yu W-P, Grunwald ME, Yau K-W. Molecular cloning, functional expression and chromosomal localization of a human homolog of the cyclic nucleotide-gated ion channel of retinal cone photoreceptors. *FEBS Lett*. 1996;393:211–215.
18. Scott S-P, Cummings J, Joe JC, Tanaka JC. Mutating three residues in the bovine rod cyclic nucleotide-activated channel can switch a nucleotide from inactive to active. *Biophys J*. 2000;78:2321–2333.
19. Gerstner A, Zong X, Hofmann F, Biel M. Molecular cloning and functional characterization of a new modulatory cyclic nucleotide-gated channel subunit from mouse retina. *J Neurosci*. 2000;20: 1324–1332.
20. Furman RE, Tanaka JC. Monovalent selectivity of the cyclic guanosine monophosphate-activated ion channel. *J Gen Physiol*. 1990;96:57–82.
21. Wissinger B, Muller F, Weyand I, et al. Cloning, chromosomal localization and functional expression of the gene encoding the α subunit of the cGMP-gated channel in human cone photoreceptors. *Eur J Neurosci*. 1997;9:2512–2521.
22. Bonigk W, Altenhofen W, Muller J, et al. Rod and cone photoreceptor cells express distinct genes for cGMP-gated channels. *Neuron*. 1993;10:865–877.
23. Weyand I, Godde M, Frings S, et al. Cloning and functional expression of a cyclic-nucleotide-gated channel from mammalian sperm. *Nature*. 1994;368:859–863.
24. Jiang Y, Lee A, Chen J, et al. X-ray structure of a voltage-dependent K^+ channel. *Nature*. 2003;423:33–41.
25. MacKenzie KR, Prestegard JH, Engleman DH. A transmembrane helix dimer: structure and implications. *Science*. 1997;276:131–133.
26. von Heijne G. Bioinformatics of membrane proteins. *Ernst Schering Res Found Workshop*. 2002;38:17–27.
27. Trudeau MC, Zagotta WN. An intersubunit interaction regulates trafficking of rod cyclic nucleotide-gated channels and is disrupted in an inherited form of blindness. *Neuron*. 2002;34:197–207.
28. Zheng J, Trudeau MC, Zagotta WN. Rod cyclic nucleotide-gated channels have a stoichiometry of three CNGA1 subunits and one CNGB1 subunit. *Neuron*. 2002;36:891–896.
29. Matulef K, Flynn GE, Zagotta WN. Molecular rearrangements in the ligand-binding domain of cyclic nucleotide-gated channels. *Neuron*. 1999;24:443–452.
30. Scott S-P, Tanaka JC. The β subunit of the cyclic nucleotide-gated channel (CNGC) confers native-like properties to the currents when co-transfected with the α subunit (abstract). *Biophys J*. 1998;74:A125.
31. Peng C, Rich ED, Varnum MD. Achromatopsia-associated mutation in the human cone photoreceptor cyclic nucleotide-gated channel CNGB3 subunit alters the ligand sensitivity and pore properties of heteromeric channels. *J Biol Chem*. 2003;278:34533–34540.
32. Faillace MP, Bernabeu RO, Korenbrot JI. Cellular processing of cone photoreceptor cyclic GMP-gated ion channels. *J Biol Chem*. 2004;279:22643–22653.
33. Chang SC, Erwin AE, Lee AS. Glucose-regulated protein (GRP94 and GRP78) genes share common regulatory domains and are coordinately regulated by common trans-acting factors. *Mol Cell Biol*. 1989;9:2153–2162.
34. Sato S, Ward CL, Krouse MEWJJ, Kopito RR. Glycerol reverses the misfolding phenotype of the most common cystic fibrosis mutation. *J Biol Chem*. 1996;271:635–638.
35. Tamarappoo BK, Yang B, Verkman AS. Misfolding of mutant aquaporin-2 water channels in nephrogenic diabetes insipidus. *J Biol Chem*. 1999;274:34825–34831.
36. Sharma M, Benharouga M, Hu W, Lukacs GL. Conformational and temperature-sensitive stability defects of the F508 cystic fibrosis transmembrane conductance regulator in post-endoplasmic reticulum compartments. *J Biol Chem*. 2001;276:8942–8950.
37. Mallouk N, Ildefonse M, Pages F, Rango M, Bennett N. Basis for intracellular retention of a human mutant of the retinal rod channel α subunit. *J Membrane Biol*. 2002;185:129–136.
38. Dryja TP, Finn JT, Peng Y, McGee TL, Berson EL, Yau K-W. Mutations in the gene encoding the alpha subunit of the rod cGMP-gated channel in autosomal recessive retinitis pigmentosa. *Proc Natl Acad Sci USA*. 1995;92:10177–10181.
39. Lukacs GL, Mohamed A, Kartner N, Chang X-B, Riordan JR, Grinstein S. Conformational maturation of CFTR but not its mutant counterpart (delta F508) occurs in the endoplasmic reticulum and requires ATP. *EMBO J*. 1994;13:6076–6086.
40. Ward CL, Kopito RR. Intracellular turnover of cystic fibrosis transmembrane conductance regulator: inefficient processing and rapid degradation of wild-type and mutant proteins. *J Biol Chem*. 1994; 269:25710–25718.
41. Cartier EA, Conti LR, Vandenberg CA, Shyng S-L. Defective trafficking and function of KATP channels caused by a sulfonylurea receptor 1 mutation associated with persistent hyperinsulinemic hypoglycemia of infancy. *Proc Natl Acad Sci USA*. 2001;98:2882–2887.
42. Zhou Z, Gong Q, January CT. Correction of defective protein trafficking of a mutant HERG potassium channel in human long QT syndrome. *J Biol Chem*. 1999;274:31123–31126.
43. Kamsteeg EJ, Wormhoudt TA, Rijss JP, van Os CH, Deen PM. An impaired routing of wild-type aquaporin-2 after tetramerization with an aquaporin-2 mutant explains dominant nephrogenic diabetes insipidus. *EMBO J*. 1999;18:2394–2400.
44. Trankner D, Jagel H, Kohl S, et al. Molecular basis of an inherited form of incomplete achromatopsia. *J Neurosci*. 2004;24:138–147.
45. Perozo E, Santacruz-Toloza L, Stefani E, Bezanilla F, Papazian DM. S4 mutations alter gating currents of Shaker K channels. *Biophys J*. 1994;66:345–354.
46. Papazian DM, Timpe LC, Jan YN, Jan LY. Alteration of voltage-dependence of Shaker potassium channel by mutations in the S4 sequence. *Nature*. 1991;349:305–310.
47. Rosenbaum T, Gordon SE. Quickening the pace: looking into the heart of HCN channels. *Neuron*. 2004;42:193–196.
48. Cuello LG, Cortes DM, Perozo E. Molecular architecture of the KvAP voltage-dependent K^+ channel in a lipid bilayer. *Science*. 2004;306:491–495.